A Fully Automatic Method to Segment Choroid Plexuses in Multiple Sclerosis Using Conventional MRI Sequences

Loredana Storelli, PhD,[1] Elisabetta Pagani, MSc,[1] Martina Rubin, MD,[1,2] Monica Margoni, MD, PhD,[1,2] Massimo Filippi, MD,[1,2,3,4,5] and Maria A. Rocca, MD[1,2,5*]

Background: Choroid plexus (CP) volume has been recently proposed as a proxy for brain neuroinflammation in multiple sclerosis (MS).
Purpose: To develop and validate a fast automatic method to segment CP using routinely acquired brain T1-weighted and FLAIR MRI.
Study Type: Retrospective.
Population: Fifty-five MS patients (33 relapsing–remitting, 22 progressive; mean age = 46.8 ± 10.2 years; 31 women) and 60 healthy controls (HC; mean age = 36.1 ± 12.6 years, 33 women).
Field Strength/Sequence: 3D T2-weighted FLAIR and 3D T1-weighted gradient echo sequences at 3.0 T.
Assessment: Brain tissues were segmented on T1-weighted sequences and a Gaussian Mixture Model (GMM) was fitted to FLAIR image intensities obtained from the ventricle masks of the SIENAX. A second GMM was then applied on the thresholded and filtered ventricle mask. CP volumes were automatically determined and compared with those from manual segmentation by two raters (with 3 and 10 years' experience; reference standard). CP volumes from previously published automatic segmentation methods (freely available Freesurfer [FS] and FS-GMM) were also compared with reference standard. Expanded Disability Status Scale (EDSS) score was assessed within 3 days of MRI. Computational time was assessed for each automatic technique and manual segmentation.
Statistical Tests: Comparisons of CP volumes with reference standard were evaluated with Bland Altman analysis. Dice similarity coefficients (DSC) were computed to assess automatic CP segmentations. Volume differences between MS and HC for each method were assessed with t-tests and correlations of CP volumes with EDSS were assessed with Pearson's correlation coefficients (R). A P value <0.05 was considered statistically significant.
Results: Compared to manual segmentation, the proposed method had the highest segmentation accuracy (mean DSC = 0.65 ± 0.06) compared to FS (mean DSC = 0.37 ± 0.08) and FS-GMM (0.58 ± 0.06). The percentage CP volume differences relative to manual segmentation were −0.1% ± 0.23, 4.6% ± 2.5, and −0.48% ± 2 for the proposed method, FS, and FS-GMM, respectively. The Pearson's correlations between automatically obtained CP volumes and the manually obtained volumes were 0.70, 0.54, and 0.56 for the proposed method, FS, and FS-GMM, respectively. A significant correlation between CP volume and EDSS was found for the proposed automatic pipeline (R = 0.2), for FS-GMM (R = 0.3) and for manual segmentation (R = 0.4). Computational time for the proposed method (32 ± 2 minutes) was similar to the manual segmentation (20 ± 5 minutes) but <25% of the FS (120 ± 15 minutes) and FS-GMM (125 ± 15 minutes) methods.
Data Conclusion: This study developed an accurate and easily implementable method for automatic CP segmentation in MS using T1-weighted and FLAIR MRI.
Evidence Level: 1
Technical Efficacy: Stage 4

J. MAGN. RESON. IMAGING 2024;59:1643–1652.

View this article online at wileyonlinelibrary.com. DOI: 10.1002/jmri.28937

Received May 18, 2023, Accepted for publication Jul 20, 2023.

*Address reprint requests to: M.A.R., Milan, Italy.
E-mail: rocca.mara@hsr.it

[Correction added on 6 October 2023, after first online publication: The copyright line was changed.]

From the [1]Neuroimaging Research Unit, Division of Neuroscience, IRCCS San Raffaele Scientific Institute, Milan, Italy; [2]Neurology Unit, IRCCS San Raffaele Scientific Institute, Milan, Italy; [3]Neurorehabilitation Unit, IRCCS San Raffaele Scientific Institute, Milan, Italy; [4]Neurophysiology Service, IRCCS San Raffaele Scientific Institute, Milan, Italy; and [5]Vita-Salute San Raffaele University, Milan, Italy

Choroid plexuses (CPs) are highly vascularized brain structures located inside the ventricular system, which are essential for the development, maintenance, and normal function of the brain and which contribute to the regulation of central nervous system (CNS) immunosurveillance.[1,2] They are responsible for cerebrospinal fluid (CSF) production, brain waste clearance pathways, including the glymphatic transport of CSF along the periarterial spaces, and for the migration of inflammatory cells within the CNS.[3,4]

CP involvement has been recently described in several neurological conditions, including multiple sclerosis (MS),[3,5–8] Alzheimer's disease,[9–11] and ischemic stroke.[12]

In MS, post-mortem studies have shown inflammatory changes within CPs, such as more antigen-presenting cells in stroma, an infiltration of peripheral leucocytes, a disruption of tight junctions in the epithelium and an endothelial overexpression of adhesion molecules involved in lymphocyte migration.[8,13,14] Notably, in experimental models, inflammation in the CPs has been observed to precede the formation of brain perivascular inflammatory infiltrates and the development of demyelinating white matter (WM) lesions.[15]

Similarly, in vivo MRI studies have demonstrated that CPs are inflamed on pseudo-T2 mapping[16] and enlarged not only in adult,[3,6,7,17] but also in pediatric[18] and presymptomatic MS patients,[19] suggesting their early involvement in the pathophysiology of the disease.

Several findings support the clinical relevance of CP enlargement in MS: higher CP volume has been shown to be significantly associated with higher Expanded Disability Status Scale (EDSS) score[20] and relapse rate, as well as with worsening of clinical disability over 5-years.[16] Enlarged CP volumes have also been correlated with several MRI measures of inflammation, including the presence of gadolinium-enhancing lesions and the number and volume of brain T2-hyperintense WM lesions.[6,7,20] More recently, CP enlargement has been correlated with the expansion of MS periventricular chronic lesions[21] and remyelination failure in periventricular areas, quantified using diffusion MRI.[22] However, the role of CP in the pathophysiology and evolution of MS needs further exploration.[5] There is growing interest in developing automatic methods for CP segmentation, to be used not only in research setting, but also in clinical trials and, ideally, in a clinic setting.[5]

Although manual segmentation is considered the reference standard for CP segmentation, it is time-consuming and prone to intra- and inter-rater variability.[23] Thus, the development of accurate automatic segmentation methods is important for studying these structures in large cohorts of subjects. The freely available and well-known software Freesurfer (FS) has been applied for this purpose[24] but it has proved to be inaccurate.[25,26] Recently, another automatic approach based on a Gaussian Mixture Model (GMM) has been proposed. Starting from FS brain tissue segmentation, this method evaluates clusters of voxel intensities in order to separate CP from CSF and ventricular wall inside the lateral ventricles.[25] This FS-GMM method has demonstrated promising results[25] on the Alzheimer's Disease Neuroimaging Initiative dataset, albeit including FS segmentation as a starting point (with a demanding requirement in terms of computational time) but studies in MS patients are lacking. Artificial intelligence segmentation techniques, especially those based on deep learning algorithms, have gained popularity in the MRI field for their very high performance in several tasks.[27] A recent study applying artificial intelligence to CP segmentation showed competitive results compared to other previously proposed deep-learning models.[28] However, this method was validated on a small cohort of patients and required a training phase on a large amount of data.

The aims of this study were to: 1) develop and validate an easily implementable fully automatic method to segment CP based on both 3D T1-weighted and 3D FLAIR brain MRI sequences, using GMM but not requiring FS segmentation as a starting point (FLAIR + T1 GMM method); and 2) to compare this approach to reference standard manual segmentation as well as to FS and its recently proposed improvement (FS-GMM method).

Materials and Methods

Ethics Committee Approval

Approval was received from the local ethical standards committee on human experimentation, and written informed consent was obtained from all subjects before MRI acquisition.

Subjects

In this retrospective study, 55 MS patients (33 relapsing–remitting and 22 progressive MS) were analyzed. To be included, patients had to have a diagnosis of MS according to the 2017 revised McDonald criteria,[29] be relapse- and steroid-free for at least 1 month prior to MRI scan, have no other relevant neurological (other than MS) or psychiatric conditions and a stable treatment for MS for at least 6 months. Sixty sex-matched healthy control (HC) subjects, without neurologic diseases or systemic disorders potentially affecting the CNS, and with a completely normal neurologic examination, were also included. Within 3 days from MRI acquisition, neurological examination, with EDSS score rating,[30] was performed by a neurologist (M.M. with 10 years' experience) blinded to the MRI findings in MS patients. Table 1 summarizes the main demographic, clinical and MRI characteristics of the study groups. Compared to HC, MS patients were significantly older.

MRI Acquisitions

Brain MRI scans were obtained using a 3.0 Tesla Philips Ingenia CX scanner (Philips Medical Systems, Best, The Netherlands) with standardized procedures for subjects positioning. The following pulse sequences were acquired (receiver Coil = dS-Head-32): sagittal 3D fluid attenuation inversion recovery (FLAIR), field of view (FOV) = 256 × 256 mm^2, pixel size = 1 × 1 mm^2, 192 slices, 1 mm slice thickness, matrix = 256 × 256, repetition time (TR) = 4800 msec, echo time (TE) = 270 msec, inversion time (TI) = 1650 msec, echo train

TABLE 1. Main Demographic, Clinical, and MRI Features of Healthy Controls and Multiple Sclerosis Patients

	HC (N = 60)	MS (N = 55)	*P*
Age, mean (SD) [years]	36.1 (12.6)	46.8 (10.2)	**<0.001**
Females/Males	33/27	31/24	0.07
Clinical phenotype (RRMS/PMS)	-	33/22	-
Disease duration, median (IQR) [years]	-	13.9 (6.0–23.0)	-
EDSS, median (IQR) [years]	-	2.5 (1.0–6.0)	-
T2-hyperintense WM lesion volume, median (IQR) [mL]	0 (0.0–0.13)	2.6 (0.93–6.6)	**<0.001**
NBV, mean (SD) [mL]	1570 (37)	1514 (53)	**<0.001**
NGMV, mean (SD) [mL]	887 (34)	848 (44)	**<0.001**
NWMV, mean (SD) [mL]	684 (29)	665 (28)	**<0.001**
NvCSFV, mean (SD) [mL]	32 (11)	45 (17)	**<0.001**

Note: Bold indicates significant values $p < 0.001$.
EDSS = Expanded Disability Status Scale; HC = healthy controls; IQR = inter-quartile range; MS = multiple sclerosis; NBV = normalized brain volume; NGMV = normalized gray matter volume; NvCSFV = normalized ventricular cerebrospinal fluid volume; NWMV = normalized white matter volume; P = progressive; RR = relapsing–remitting; SD = standard deviation.

length (ETL) = 167, acquisition time (TA) = 6.15 minutes; sagittal 3D T1-weighted magnetization-prepared rapid gradient-echo (MPRAGE), FOV = 256 × 256 mm^2, pixel size = 1 × 1 mm^2, 204 slices, 1 mm slice thickness, matrix = 256 × 256, TR = 7 msec, TE = 3.2 msec, TI = 1000 msec, flip angle = 8°, TA = 8.53 minutes.

MRI Pre-Processing

All sagittal acquisitions were reoriented to the axial plane and the portion of the neck extending below the cerebellum was cropped for both FLAIR and 3D T1-weighted sequences. Focal brain T2-hyperintense WM lesions were identified and segmented by a fully automated deep-learning approach using co-registered 3D FLAIR and 3D T1-weighted images as inputs.[31] Then, brain T2-hyperintense WM lesion volume (LV) was obtained for each participant from their lesion masks.

Brain tissues were automatically segmented on 3D T1-weighted sequences, after lesion-filling,[32] to obtain gray matter (GM), WM, and CSF masks using FSL-SIENAX toolbox, and their associated normalized brain, GM and WM volumes were measured.[33]

Manual Choroid Plexuses Segmentation

For all subjects, CPs of the lateral ventricles were manually segmented in the sagittal, axial, and coronal planes of the 3D T1-weighted sequence using a local thresholding segmentation technique (Jim 8.0, Xinapse Systems Ltd, Colchester, UK) by two raters (M.M. and M.R. with 10- and 3-years' experience). The CPs of the third and fourth ventricles were not included in the segmentation, given their variable visualization.[34] First, to evaluate intra-observer and inter-observer reproducibility, CPs of 10 randomly selected subjects (5 HC and 5 patients with MS) were segmented by both raters twice, with an interval of at least 15 days between the two assessments. Intraclass correlation coefficient (ICC) was used to estimate reliability, using a two-way mixed model for the inter-rater reliability and a one-way random model for the intra-rater reliability (first operator intra-rater ICC = 0.962; second operator intra-rater ICC = 0.988; inter-rater ICC = 0.923; all significant). Subsequently, the two raters performed CP segmentation separately.

Manual segmentation was considered the reference standard to compare all the automatic methods presented in this study. All the obtained CP volumes were multiplied by V scaling (derived from the FSL-SIENAX toolbox, as a measure of head size) to obtain the corresponding normalized values.[7]

Automatic Choroid Plexuses Segmentation

The proposed fully automatic method to segment CPs started from the brain tissue segmentation obtained from the FSL-SIENAX toolbox (as described in the previous paragraph). In particular, the mask of the lateral ventricle in the standard MNI-152 atlas space[35] was affinely registered into the subject space and subsequently eroded, with a dimension of the filter = 1 mm to clean the mask without erasing relevant part of brain tissue. The co-registered mask of the lateral ventricle was then used as a template to separate peripheral from ventricular CSF for each subject on the global CSF segmentation. Then, we removed on the previously obtained lateral ventricle binary mask of each subject those voxels with a high probability (>50%) to belong to other tissues (GM, WM, or T2-hyperintense lesions), as indicated from the SIENAX segmentation. Thus, we reduced the numbers of possible outliers on the lateral ventricle masks that could have image intensities similar to those of the CPs

on the FLAIR images. The resulting "cleaned" ventricle mask was registered into the FLAIR space and the corresponding image intensities were extracted. Since CPs appear hyperintense on FLAIR images and the signal of the CSF is suppressed, a GMM with 2 Gaussian distributions was fitted to data using the iterative Expectation–Maximization algorithm.[36] The voxels belonging to the Gaussian distribution with lower image intensities (CSF) were discarded. A mean image filtering was applied on the previously obtained binary mask to enhance the differences between voxels belonging to the CPs and spurious boundary voxels. A second GMM, again with two Gaussian distributions, was applied on the filtered binary mask and residual clusters of voxels with a dimension <3 mm in all three dimensions were removed. The resulting mask was the final CP segmentation. The segmentation algorithm was implemented in Matlab (R2017a, Mathworks) and is schematically represented in Fig. 1.

The proposed method was compared with automatic CP segmentation from FS[24] and with a recently published algorithm for automatic CP segmentation that starts from FS segmentation (freely available for download on github at https://github.com/EhsanTadayon/choroid-plexus-segmentation).[25] Pre-processed 3D T1-weighted sequences were used as input for both methods.

Statistical Analysis

Demographic, clinical, and MRI measures were compared between groups (HC and MS) using Pearson's χ^2 test for categorical variables and Mann–Whitney or *t*-test for continuous variables (after assessing normality of the distributions).

For all subjects, segmentation accuracy of the three automatic pipelines was evaluated using the Dice similarity coefficient (DSC) and compared using paired *t*-tests. Dice coefficients will be defined as low (0.00–0.19), low-moderate (0.20–0.39), moderate (0.40–0.59), moderate-high (0.60–0.79) or high (0.80–1.00). Automatic CP volume differences and Pearson's correlations (coefficient *R*) with the manually obtained CP volumes were used to assess and compare the performance of the three automatic methods.

Between-group differences (HC vs. MS) in CP volumes for the different segmentation pipelines were also assessed in comparison to the between-group difference for the manually extracted CP volumes. For MS patients, Spearman's partial

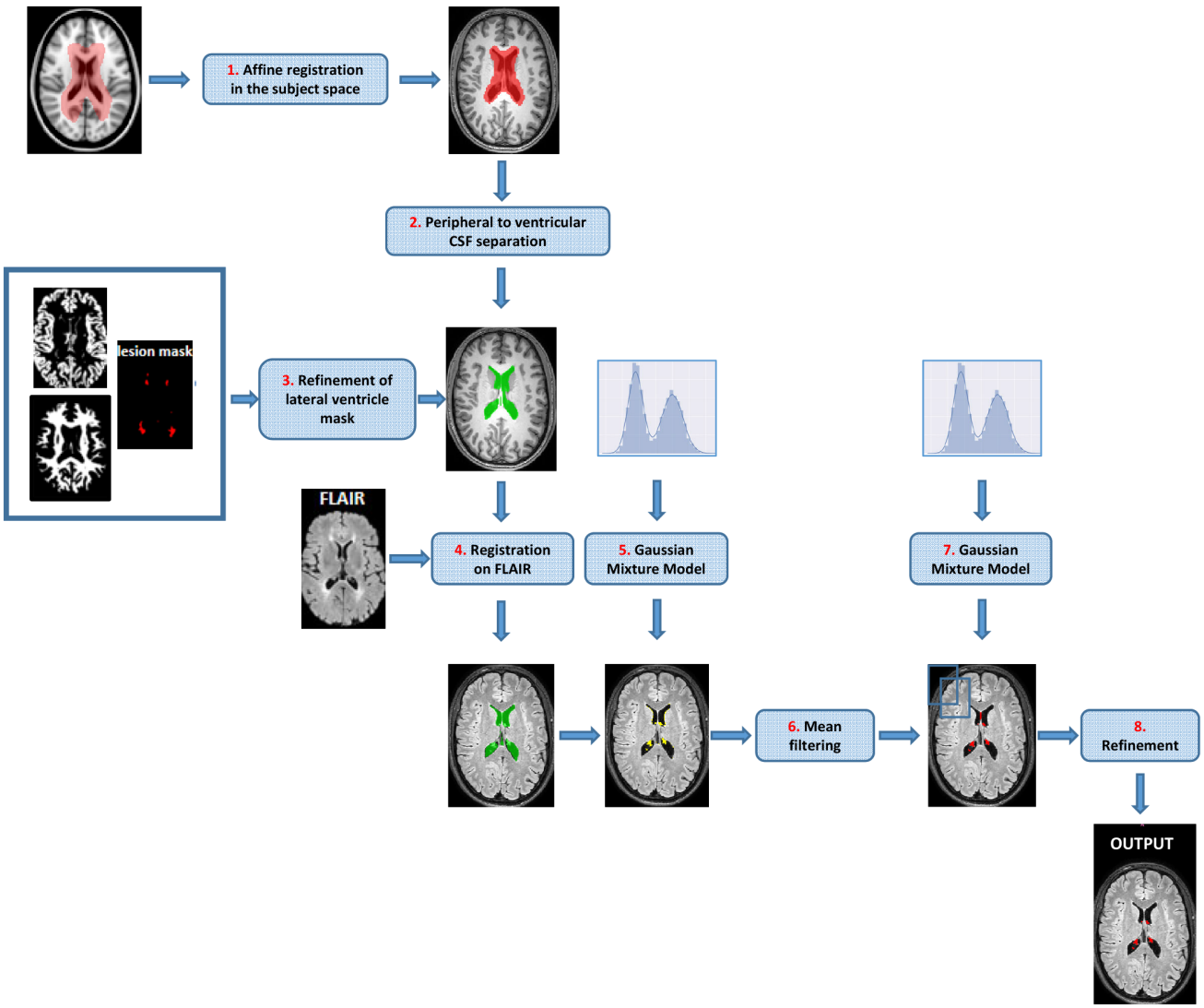

FIGURE 1: A schematic overview of the implemented method for the automatic segmentation of choroid plexuses. CSF = cerebrospinal fluid.

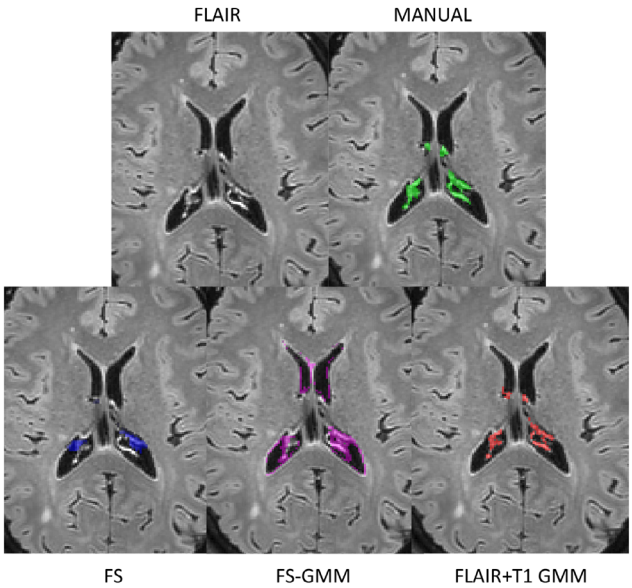

FIGURE 2: Examples of choroid plexus segmentation. In the first row, an axial slice from a FLAIR sequence obtained from a multiple sclerosis patient with manual choroid segmentation (in green). In the second row, the three automatic segmentation masks with different colors: Freesurfer (FS) in blue, the recently published FS extension in magenta (FS-GMM) and the proposed method in red (FLAIR + T1 GMM). FS = Freesurfer; GMM = Gaussian Mixture Model.

correlations (age-adjusted) of normalized CP volumes with brain T2-hyperintense WM LV and EDSS were calculated. We also analyzed the time required for CP segmentation from the three automated methods.

False discovery rate (Benjamini–Hochberg procedure) correction was applied for multiple comparisons. A P-value <0.05 was considered significant. R software (version 4.0.5) and Matlab (R2017a, Mathworks) were used for statistical analysis.

Data and Code Availability Statement

The code will be made available upon reasonable request to the corresponding author.

Results

Clinical and MRI Findings

Compared to HC, MS patients had significantly higher brain T2-hyperintense WM LV and larger ventricular CSF volume, and significantly lower normalized brain, GM and WM volumes.

Segmentation Accuracy

Figure 2 shows an example of segmentation with the automatic methods tested.

Compared to manual segmentation, the FLAIR + T1 GMM method showed moderate-high segmentation accuracy with a mean DSC score of 0.66 (±0.04) for HC and 0.63 (±0.08) for MS patients. Significantly lower DSC were found for both FS (low-moderate DSC = 0.37 ± 0.07 for HC and DSC = 0.37 ± 0.08 for MS) and FS-GMM methods

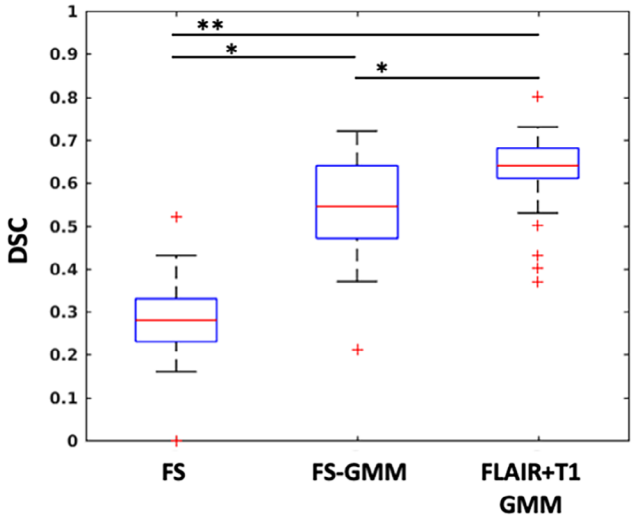

FIGURE 3: Boxplot of Dice similarity coefficients obtained for the three automatic methods for all subjects' choroid plexus segmentations (FS, FS-GMM, FLAIR + T1 GMM). Significant differences between the methods were highlighted (*P < 0.05; **P < 0.001). DSC = dice similarity coefficient; FS = Freesurfer; GMM = Gaussian Mixture Model.

(moderate DSC = 0.60 ± 0.05 for HC and DSC = 0.56 ± 0.06 for MS) in comparison to FLAIR + T1 GMM method, as shown in Fig. 3.

The CP volumes estimated with the FLAIR + T1 GMM method were not significantly different to the manually estimated volumes (−0.1% ± 0.23%, P = 0.32) (Fig. 4). The mean percentage differences between CP volumes obtained by FS and FS-GMM methods compared to manually extracted volumes (Fig. 4) were statistically significant (4.6% ± 2.5 and −0.48 ± 2, respectively).

Pearson's correlations between automatically obtained CP volumes and those obtained from the manual segmentation were 0.70, 0.54, and 0.56 (all significant) for the proposed method, FS, and FS-GMM, respectively (Fig. 5).

There was significantly higher CP volume in MS patients (1.46 ± 0.31 mL) than HC (1.39 ± 0.30 mL) from manual segmentation. For the automatic pipelines, there were significant differences between HC and MS CP volumes for the proposed method (HC = 1.28 ± 0.32 mL, MS = 1.50 ± 0.42 mL), for FS (HC = 0.74 ± 0.23 mL, MS = 1.38 ± 0.42 mL) and for FS-GMM (HC = 1.24 ± 0.25 mL, MS = 1.80 ± 0.42 mL) (Table 2).

Correlations With MRI and Clinical Measures

Table 3 summarizes results of analysis of correlations.

No significant correlation was observed between normalized CP volumes and brain T2-hyperintense WM LV in MS patients for both manual segmentation (P = 0.53) and our proposed method (P = 0.62). Conversely, a significant association between the normalized CP volumes and brain

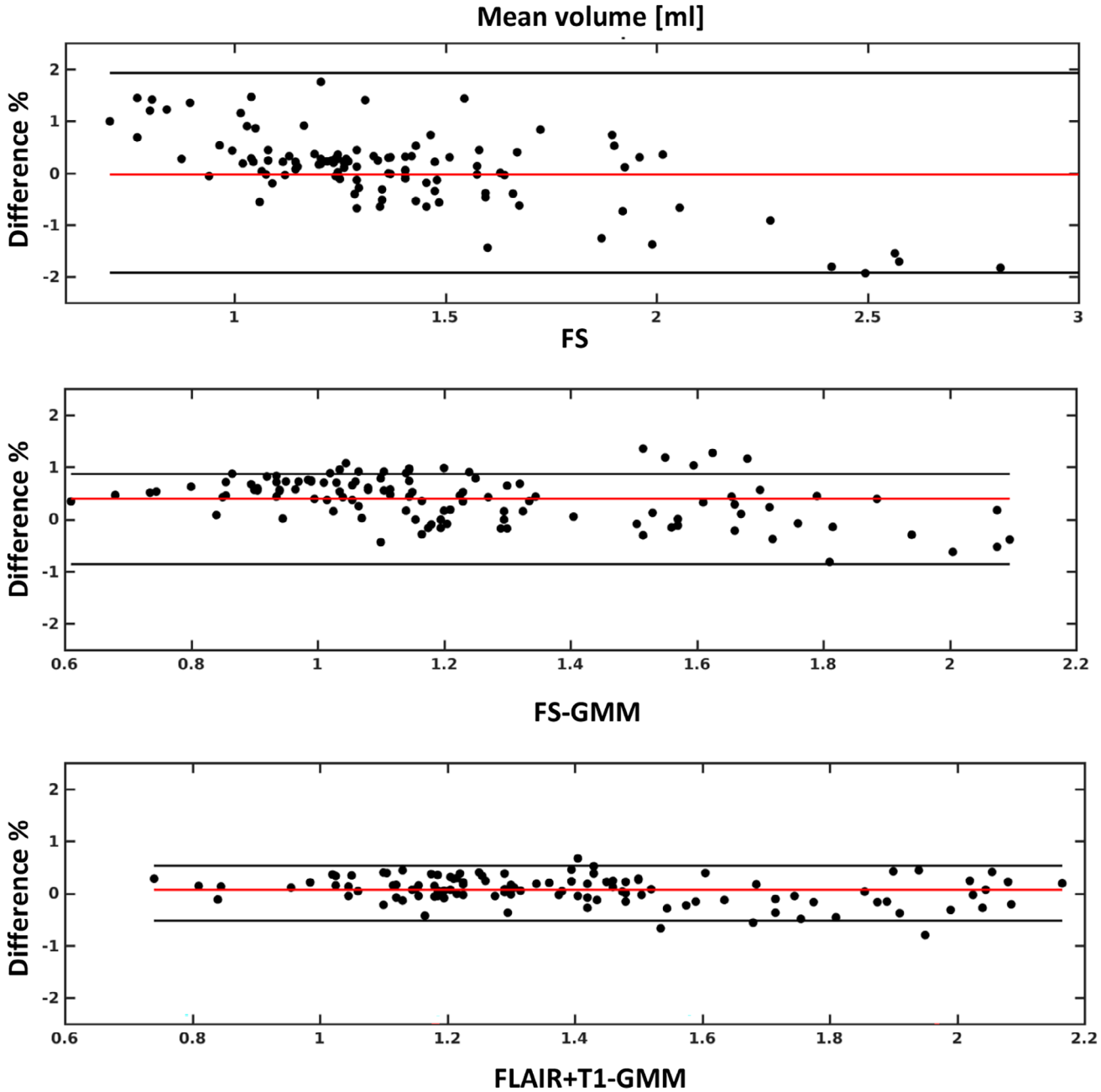

FIGURE 4: Bland–Altman plots of the volume percentage differences obtained from the automatic choroid plexus segmentation methods compared to manually obtained volumes, for all the enrolled subjects. FS = Freesurfer; GMM = Gaussian Mixture Model; mL = milliliter.

T2-hyperintense WM LV in MS patients was found for both FS ($R = 0.3$) and FS-GMM ($R = 0.6$) methods.

In MS patients, a significant correlation between CP volumes and EDSS was observed for manual segmentation ($R = 0.4$), FLAIR + T1 GMM pipeline ($R = 0.2$) and FS-GMM methods ($R = 0.3$). CP volumes obtained from FS segmentation did not show a significant association with EDSS score ($P = 0.71$).

The proposed automated method was the fastest automatic CP segmentation method (approximately 2 minutes + 30 minutes for SIENAX brain tissues segmentation per subject) with a 75% analysis time reduction compared to FS (around 2 hours per subject) and FS-GMM (around 5 minutes + 2 hours for FS tissues segmentation per subject) methods, running on a computer with an Intel Xeon 12 core processor (Intel, Santa Clara, California; USA), 16Gb RAM and a Quadro K600 GPU (NVIDIA, Santa Clara, California; USA), with CentOS Linux 7. Mean computational time for the manual segmentation was 20 ± 5 minutes, 32 ± 2 minutes for the proposed method, 120 ± 15 minutes for FS, and 125 ± 15 minutes for FS-GMM method.

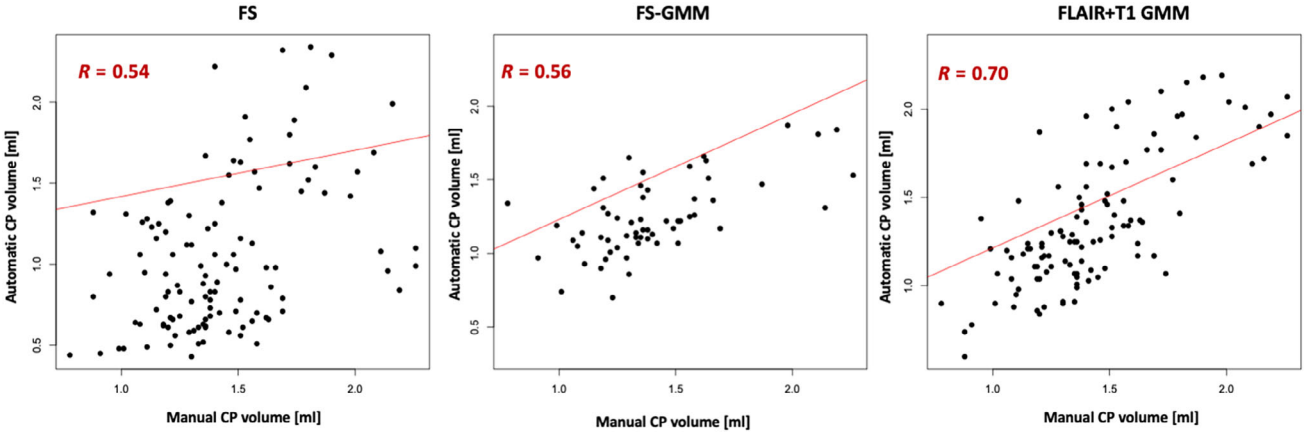

FIGURE 5: Scatter plots with correlations between automatically obtained choroid plexuses volumes and those obtained from the manual segmentation. Pearson's correlations results (*R*) were also highlighted in red. CP = choroid plexus; FS = Freesurfer; GMM = Gaussian Mixture Model.

TABLE 2. Normalized Choroid Plexus Volume in Healthy Controls and Multiple Sclerosis Patients With the Application of Different Methods

	HC (N = 60)	MS (N = 55)	*P*
Manual segmentation, mean (SD)	1.39 (0.30)	1.46 (0.31)	<0.05
In-house method, mean (SD)	1.28 (0.32)	1.50 (0.42)	<0.001
FS, mean (SD)	0.74 (0.23)	1.38 (0.42)	<0.001
FS-GMM, mean (SD)	1.24 (0.25)	1.80 (0.42)	<0.001

HC = healthy controls; FS = FreeSurfer; GMM = Gaussian mixture model; MS = multiple sclerosis; SD = standard deviation.

Discussion

In this study, we proposed a fully automatic method for CP segmentation and volume estimation for MS patients using two conventionally acquired MRI sequences (3D T1-weighted and FLAIR images). The method implemented resulted in CP volumes with small percentage differences compared to reference standard manual segmentation, and high Dice scores. The performance of the proposed FLAIR + T1 GMM method was better than FS and a recently proposed automatic toolbox that includes FS segmentation of brain tissues (FS-GMM) methods.[25]

There is growing interest in studying CP in MS patients as a possible biomarker of brain inflammation.[8,13–15] However, manual segmentation of this structure on MRI is time-consuming and prone to intra- and inter-observer variability, thus discouraging its study on large samples of patients. Previous imaging studies have used FS, a freely available toolbox, for automatic segmentation of the CPs.[25,26,37] However, from a quality control of the results and consistent with previous studies,[25,26] FS is inaccurate for this specific brain structure. In particular, it often missed the majority of the CP within right lateral ventricle (as in Fig. 2) and mislabelled CSF voxels as CP voxels. A potential cause of the lack of good segmentation accuracy for FS could be due to the fixed constraints imposed by the atlas-based segmentation and to possible morphometric distortions due to registration inaccuracies. For this

TABLE 3. Spearman's Partial Correlations (Age-Adjusted) of Normalized CP Volumes With Brain T2-Hyperintense WM Lesion Volume and EDSS in MS Patients, for All the Segmentation Methods.

Spearman's Partial Correlations, *R* (p)	Brain T2-Hyperintense WM Lesion Volume	EDSS
Manual segmentation	0.2 (0.09)	**0.4 (0.007)**
FS	**0.3 (0.05)**	0.2 (0.18)
FS + GMM	**0.6 (<0.001)**	**0.3 (0.01)**
FLAIR + T1 GMM	0.2 (0.07)	**0.2 (0.03)**

Bold text is for significant correlations. CP = choroid plexus; EDSS = Expanded Disability Status Scale; FS = FreeSurfer; GMM = Gaussian mixture model; MS = multiple sclerosis; WM = white matter.

reason, a new automatic tool that improves FS segmentation of CPs using GMM has been recently proposed and validated (FS-GMM).[25] New segmentation algorithms using artificial intelligence techniques, such as deep learning, have also recently gained popularity for their high performance,[27] with several being developed for automatic CP segmentation.[26,28,38] However, these techniques require large amounts of labeled data for training and high computational performance with dedicated hardware,[39] making them ungeneralizable and difficult to apply in clinical practice.

We implemented an automatic method for CP segmentation in MS, based on two conventional MRI sequences (3D T1-weighted and 3D FLAIR) which did not involve a training step (as in deep-learning algorithms), nor a demanding brain tissue segmentation step as a starting point for the algorithm (as for FS-GMM method).

We compared the performance of our method with manual segmentation performed by two raters and with the two available automatic algorithms for CP segmentation (FS and FS-GMM). In the comparison with manual segmentation, our method showed highest segmentation accuracy in terms of spatial overlap (DSC) between the two segmentation masks and volumetric similarity, with slightly better performance in HC than in MS patients. Conversely, in line with the literature, FS segmentation of CPs showed the lowest similarity with manual segmentation, which improved when using the recently proposed FS-GMM method. In this comparison, our method also significantly outperformed FS-GMM in terms of segmentation accuracy (DSC) and volume similarity (as shown by the Pearson's correlations), even though both methods are based on GMM and intensity outliers' detection. This could be due to the fact that the FS-GMM method, even if it improves CP segmentation in comparison to the original FS method, still includes as a first step the brain tissue masks produced by FS. Thus, if there are inaccuracies in the segmentation of brain tissue structures (for example the ventricle mask) these will be present in the starting point masks for FS-GMM.

Consistent with previous studies,[6–8,17,18] all pipelines showed a significant enlargement of CP volume in MS patients compared to HC. However, the FLAIR + T1 GMM method showed the closest agreement with the results of manual segmentation both in HC and MS patients. The largest difference between HC and MS CP volumes was observed with FS segmentations, followed by FS-GMM method, confirming a less accurate performance compared to manual segmentation. The larger group differences found with the Freesurfer-based methods could be due to disease-specific features of MS patients. Indeed, FS method included an atlas-based segmentation that preserves anatomical commonalities across subjects in the expense of losing peculiarities for each subject.[25] Thus, by imposing a fixed constraint, a larger lateral ventricle due to the pathological brain atrophy occurring in these patients could reduce the level of FS segmentation accuracy.

Finally, we assessed the performance of our method by evaluating the association between CP volumes and clinical measures, considering the results obtained from the manual segmentation method as a reference. Similarly to the manual segmentation, but differently from FS and FS-GMM, our approach showed no significant association between CP volume and brain T2-hyperintense WM LV. When considering the association between CP volumes and EDSS score, both our algorithm and the FS-GMM method showed a significant positive correlation, as for the results obtained from the manual segmentation by raters (our reference standard).

These findings support the use of our novel approach as a reliable method to evaluate the clinical relevance of CP volume, promoting its application in larger MS studies. It has the important benefit of reducing processing time compared to FS-GMM (by approximately 75%), since there is no need for prior FS segmentation, is easy to implement and does not involve an initial training phase on large amounts of labeled data. It is therefore generalizable and is a simple tool that may potentially be integrated in a clinical setting.

Limitations

Although this study has a cross-sectional design, different studies have demonstrated a good intra- and inter-rater reproducibility in the manual segmentation of CPs.[7] However, future longitudinal studies are needed to prove the robustness and reliability of the proposed CP segmentation algorithm on serial MRI visits and to explore the dynamic abnormalities of these structures over time. Second, the Dice coefficients obtained with the proposed CP segmentation are in the moderate range. However, this is what we expect by using Dice metric to assess segmentation performance on small structures. In these cases, Dice coefficient may not be the appropriate metric, since a single-pixel difference between two predictions can have a large impact on the metric values. Nevertheless, this is the most commonly used metric in literature to evaluate image segmentation performance. Finally, the segmentation results may depend on the image quality. The acquisition of 3D data is therefore desirable in terms of higher signal-to-noise ratio and tissue contrast, in order to obtain a good model of the Gaussian distributions of the image intensities of the structures to separate (lateral ventricle and CP). The method is therefore based on 3D sequences usually acquired in a clinical setting (T1-weighted and FLAIR), since the consensus recommendations on the use of MRI in MS are encouraging the acquisition of high-resolution images.[40]

Conclusions

We developed an accurate and easily implementable method for fully automatic CP segmentation in MS patients using

3D T1-weighted and FLAIR brain MRI sequences. This algorithm allows a rapid quantification of CP volume, a possible clinically relevant measure of brain inflammation in MS patients.

Acknowledgment

Open access funding provided by BIBLIOSAN.

Conflict of Interest

Loredana Storelli received grants and contracts from FISM – Fondazione Italiana Sclerosi Multipla – within a fellowship program (cod. 2019/BR/009) and received speakers' honoraria from Biogen. Elisabetta Pagani received speakers' honoraria from Biogen Idec. Martina Rubin has nothing to disclose. Monica Margoni was awarded a MAGNIMS-ECTRIMS fellowship in 2020. Prof. Massimo Filippi is Editor-in-Chief of the Journal of Neurology, Associate Editor of Human Brain Mapping, Neurological Sciences, and Radiology; received compensation for consulting services from Alexion, Almirall, Biogen, Merck, Novartis, Roche, Sanofi; speaking activities from Bayer, Biogen, Celgene, Chiesi Italia SpA, Eli Lilly, Genzyme, Janssen, Merck-Serono, Neopharmed Gentili, Novartis, Novo Nordisk, Roche, Sanofi, Takeda, and TEVA; participation in Advisory Boards for Alexion, Biogen, Bristol-Myers Squibb, Merck, Novartis, Roche, Sanofi, Sanofi-Aventis, Sanofi-Genzyme, Takeda; scientific direction of educational events for Biogen, Merck, Roche, Celgene, Bristol-Myers Squibb, Lilly, Novartis, Sanofi-Genzyme; he receives research support from Biogen Idec, Merck-Serono, Novartis, Roche, Italian Ministry of Health, and Fondazione Italiana Sclerosi Multipla. Prof. Maria A. Rocca received consulting fees from Biogen, Bristol Myers Squibb, Eli Lilly, Janssen, Roche; and speaker honoraria from AstraZaneca, Biogen, Bristol Myers Squibb, Bromatech, Celgene, Genzyme, Horizon Therapeutics Italy, Merck Serono SpA, Novartis, Roche, Sanofi and Teva. She receives research support from the MS Society of Canada, the Italian Ministry of Health, and Fondazione Italiana Sclerosi Multipla. She is Associate Editor for Multiple Sclerosis and Related Disorders.

References

1. Benarroch EE. Choroid plexus—CSF system: Recent developments and clinical correlations. Neurology 2016;86(3):286-296.
2. Ghersi-Egea JF, Strazielle N, Catala M, Silva-Vargas V, Doetsch F, Engelhardt B. Molecular anatomy and functions of the choroidal blood-cerebrospinal fluid barrier in health and disease. Acta Neuropathol 2018;135(3):337-361.
3. Vercellino M, Votta B, Condello C, et al. Involvement of the choroid plexus in multiple sclerosis autoimmune inflammation: A neuropathological study. J Neuroimmunol 2008;199(1–2):133-141.
4. Kooij G, Kopplin K, Blasig R, et al. Disturbed function of the blood-cerebrospinal fluid barrier aggravates neuro-inflammation. Acta Neuropathol 2014;128(2):267-277.
5. Muller J, Noteboom S, Granziera C, Schoonheim MM. Understanding the role of the choroid plexus in multiple sclerosis as an MRI biomarker of disease activity. Neurology 2023;100(9):405-406.
6. Muller J, Sinnecker T, Wendebourg MJ, et al. Choroid plexus volume in multiple sclerosis vs neuromyelitis optica spectrum disorder: A retrospective, cross-sectional analysis. Neurol Neuroimmunol Neuroinflamm 2022;9(3):e1147.
7. Ricigliano VAG, Morena E, Colombi A, et al. Choroid plexus enlargement in inflammatory multiple sclerosis: 3.0-T MRI and translocator protein PET evaluation. Radiology 2021;301(1):166-177.
8. Rodriguez-Lorenzo S, Konings J, van der Pol S, et al. Inflammation of the choroid plexus in progressive multiple sclerosis: Accumulation of granulocytes and T cells. Acta Neuropathol Commun 2020;8(1):9.
9. Municio C, Carrero L, Antequera D, Carro E. Choroid plexus aquaporins in CSF homeostasis and the glymphatic system: Their relevance for Alzheimer's disease. Int J Mol Sci 2023;24(1):878.
10. Serot JM, Bene MC, Faure GC. Choroid plexus, aging of the brain, and Alzheimer's disease. Front Biosci 2003;8:s515-s521.
11. Tadayon E, Pascual-Leone A, Press D, Santarnecchi E. Alzheimer's disease neuroimaging I. choroid plexus volume is associated with levels of CSF proteins: Relevance for Alzheimer's and Parkinson's disease. Neurobiol Aging 2020;89:108-117.
12. Egorova N, Gottlieb E, Khlif MS, Spratt NJ, Brodtmann A. Choroid plexus volume after stroke. Int J Stroke 2019;14(9):923-930.
13. Thompson D, Brissette CA, Watt JA. The choroid plexus and its role in the pathogenesis of neurological infections. Fluids Barriers CNS 2022;19(1):75.
14. Wilson EH, Weninger W, Hunter CA. Trafficking of immune cells in the central nervous system. J Clin Invest 2010;120(5):1368-1379.
15. Brown DA, Sawchenko PE. Time course and distribution of inflammatory and neurodegenerative events suggest structural bases for the pathogenesis of experimental autoimmune encephalomyelitis. J Comp Neurol 2007;502(2):236-260.
16. Bergsland N, Dwyer MG, Jakimovski D, et al. Association of choroid plexus inflammation on MRI with clinical disability progression over 5 years in patients with multiple sclerosis. Neurology 2023;100(9):e911-e920.
17. Kim H, Lim YM, Kim G, et al. Choroid plexus changes on magnetic resonance imaging in multiple sclerosis and neuromyelitis optica spectrum disorder. J Neurol Sci 2020;415:116904.
18. Margoni M, Gueye M, Meani A, et al. Choroid plexus enlargement in paediatric multiple sclerosis: Clinical relevance and effect of sex. J Neurol Neurosurg Psychiatry 2023;94(3):181-188.
19. Ricigliano VAG, Louapre C, Poirion E, et al. Imaging characteristics of choroid plexuses in presymptomatic multiple sclerosis: A retrospective study. Neurol Neuroimmunol Neuroinflamm 2022;9(6):e200026.
20. Fleischer V, Gonzalez-Escamilla G, Ciolac D, et al. Translational value of choroid plexus imaging for tracking neuroinflammation in mice and humans. Proc Natl Acad Sci U S A 2021;118(36):e2025000118.
21. Klistorner S, Barnett MH, Parratt J, Yiannikas C, Graham SL, Klistorner A. Choroid plexus volume in multiple sclerosis predicts expansion of chronic lesions and brain atrophy. Ann Clin Transl Neurol 2022;9(10):1528-1537.
22. Tonietto M, Poirion E, Lazzarotto A, et al. Periventricular remyelination failure in multiple sclerosis: A substrate for neurodegeneration. Brain 2023;146(1):182-194.
23. Muthuraman M, Oshaghi M, Fleischer V, et al. Choroid plexus imaging to track neuroinflammation – a translational model for mouse and human studies. Neural Regen Res 2023;18(3):521-522.
24. Fischl B, Salat DH, Busa E, et al. Whole brain segmentation: Automated labeling of neuroanatomical structures in the human brain. Neuron 2002;33(3):341-355.
25. Tadayon E, Moret B, Sprugnoli G, et al. Improving choroid plexus segmentation in the healthy and diseased brain: Relevance for tau-PET imaging in dementia. J Alzheimers Dis 2020;74(4):1057-1068.

26. Zhao LFX, Meyer C, Alsop DC. Choroid plexus segmentation using optimized 3D U-net. In: Society IC, editor. *2020 IEEE 17th International Symposium on Biomedical Imaging (ISBI)*. Iowa City, IA, USA: IEEE; 2020. p 381-384.

27. Hesamian MH, Jia W, He X, Kennedy P. Deep learning techniques for medical image segmentation: Achievements and challenges. J Digit Imaging 2019;32(4):582-596.

28. Schmidt-Mengin M, Ricigliano VAG, Bodini B, et al. Axial multi-layer perceptron architecture for automatic segmentation of choroid plexus in multiple sclerosis. Proc. SPIE 12032, Medical Imaging 2022: Image Processing, 1203208; 2022.

29. Thompson AJ, Banwell BL, Barkhof F, et al. Diagnosis of multiple sclerosis: 2017 revisions of the McDonald criteria. Lancet Neurol 2018; 17(2):162-173.

30. Kurtzke JF. Rating neurologic impairment in multiple sclerosis: An expanded disability status scale (EDSS). Neurology 1983;33(11):1444-1452.

31. Valverde S, Cabezas M, Roura E, et al. Improving automated multiple sclerosis lesion segmentation with a cascaded 3D convolutional neural network approach. Neuroimage 2017;155:159-168.

32. Battaglini M, Jenkinson M, De Stefano N. Evaluating and reducing the impact of white matter lesions on brain volume measurements. Hum Brain Mapp 2012;33(9):2062-2071.

33. Smith SM, Zhang Y, Jenkinson M, et al. Accurate, robust, and automated longitudinal and cross-sectional brain change analysis. Neuroimage 2002;17(1):479-489.

34. Horsburgh A, Kirollos RW, Massoud TF. Bochdalek's flower basket: Applied neuroimaging morphometry and variants of choroid plexus in the cerebellopontine angles. Neuroradiology 2012;54(12):1341-1346.

35. Evans AC, Collins DL, Millst SR, Brown ED, Kelly RL, Peters TM. 3D statistical neuroanatomical models from 305 MRI volumes. In: IEEE, editor. *1993 IEEE Nuclear Science Symposium and Medical Imaging Conference*. San Francisco, CA, USA: IEEE; 1993. p 1813-1817.

36. Balafar MA. Gaussian mixture model based segmentation methods for brain MRI images. Artif Intell Rev 2012;41:429-439.

37. Fischl B. FreeSurfer. Neuroimage 2012;62(2):774-781.

38. Yazdan-Panah A, Schmidt-Mengin M, Ricigliano VAG, Soulier T, Stankoff B, Colliot O. Automatic segmentation of the choroid plexuses: method and validation in controls and patients with multiple sclerosis. NeuroImage: Clinical 2023;38:103368.

39. Kim M, Yun J, Cho Y, et al. Deep learning in medical imaging. Neurospine 2019;16(4):657-668.

40. Wattjes MP, Ciccarelli O, Reich DS, et al. 2021 MAGNIMS-CMSC-NAIMS consensus recommendations on the use of MRI in patients with multiple sclerosis. Lancet Neurol 2021;20(8): 653-670.